JERZY KRUKOWSKI [*], *ANDRZEJ MACZYŃSKI* [**]

APPLICATION OF THE RIGID FINITE ELEMENT METHOD FOR MODELLING AN OFFSHORE PEDESTAL CRANE

In offshore pedestal cranes one may distinguish three components of considerable length: a pedestal, a boom and a frame present in some designs. It is often necessary in dynamical analyses to take into account their flexibility. A convenient and efficient method for modelling them is the rigid finite element method in a modified form. The rigid finite element method allows us to take into account the flexibility of the beam system in selected directions while introducing a relatively small number of additional degrees of freedom to the system. This paper presents a method for modelling the pedestal, the frame and the boom of an offshore column crane, treating each of these components in a slightly different way. A custom approach is applied to the pedestal, using rigid finite elements of variable length. Results of sample numeric computations are included.

1. Introduction

MRFEM, a modified form of the rigid finite element method, allows one to conveniently model flexibility of beam components of multicomponent systems, while introducing a relatively small number of additional degrees of freedom. It enables modelling flexural flexibility in two planes and torsional flexibility. Depending on the system's features, the model may be easily limited to the dominant flexibility, thus further reducing its number of degrees of freedom.

Extraction of undersea natural resources, particularly oil and gas, has expedited the significant progress in offshore technology for last few decades. Various types of cranes are an important aid in the construction of extraction

---

[*] *National Oilwell Varco Poland, Arkońska 6, 80-387 Gdańsk, Poland; E-mail: Jerzy.Krukowski@nov.com*

[**] *University of Bielsko-Biała, Faculty of Mechanical Engineering and Computer Sciences, Willowa 2, 43-309 Bielsko-Biała, Poland; E-mail: amaczynski@ath.eu*

infrastructure as well as its operation and servicing. Reloading and assembly works realised using various types of cranes are among widely performed and highly important operations in offshore engineering. One of the main features distinguishing offshore cranes from the land ones are significant movements of the base caused by sea waves. In the case whereby, a load is lifted from a supply ship also the load is in such motion. Taking the criterion of construction into account, one may distinguish the following types of offshore cranes:

- A-frames,
- gantries,
- boom cranes.

Issues related to the dynamic analysis of offshore cranes are naturally subject to a number of scientific papers. A-frames were among others considered in [1, 2]. A mathematical model of a gantry BOP crane, installed on the oil platform, was presented in [3]. Nonlinear dynamic response to a regular waving of a crane mounted on the vessel was examined in [4, 5]. Operation of a winch in order to limit overload of a system or vertical movements of a load caused by the sea waving was considered in [6]. Mechanical anti–pendulum system was presented in [7]. Reduction of load swinging via proper steering of crane slew and boom hoist was considered in [8, 9]. A different concept of stabilizing the load position of an offshore crane was the subject of [10]. Two different algorithms of control that minimizes load waving were discussed in [11].

The subject of this paper is the offshore pedestal crane with a rope overhang control system and a truss or box boom – Fig. 1. The mentioned advantages of the rigid finite element method in its modified form gave the authors incentive to try applying it to modelling a crane. In cranes of this type, three main components of considerable length may be distinguished: a pedestal, a boom and a frame. Their structure allows them to be treated as beam components. Additionally, in each case (the pedestal, the frame, and the boom) the flexibilities having the most influence on the entire crane's dynamics can be distinguished.

Experience of engineers working for National Oilwell Varco shows that, for the pedestal, the main role in dynamical analyses plays the effect of inclination of its upper plane. Therefore, in addition to the classical approach to modelling which uses the rigid finite element method, a custom one is also proposed, introducing rigid finite elements of variable length. It is discussed in chapter 4.

The frame's height is often of several metres, and the inclination of its upper part in the plane containing the frame can well reach 100 mm. The deflections are much smaller in the perpendicular plane. The flexural

Fig. 1. Offshore pedestal crane[1]

flexibility is therefore considered in the former plane only. Omitting the flexural and torsional flexibility in the latter plane allows us to reduce the number of the model's degrees of freedom significantly.

On the other hand, the boom is modelled classically. The computer programme is developed also to support the ability to treat the considered components of a crane as rigid ones. This makes it possible to observe the influence of flexibilities of particular sets of components on the dynamics of the entire crane by case analysis, whereby some are treated as rigid and others as flexible.

2. Model of an offshore pedestal crane

The scheme of the model of an offshore pedestal crane is shown in Fig. 2. The following assumptions are taken into consideration:

---

[1] The picture is used by permission from National Oilwell Varco

- The base of the crane (a platform or a vessel) and the supply vessel are rigid bodies with 6 degrees of freedom. The movement is caused by waving defined by pseudo-harmonic functions.
- The pedestal, the frame and the boom are modelled by means of the Rigid Finite Element Method using a modified approach (MRFEM) [12].
- The king frame, including the slewing part, is treated as a rigid structure with one degree of freedom with respect to the pedestal – the slew angle.
- The hoist and the luffing ropes are modelled as a massless element with equivalent longitudinal flexibility. The damping is taken into account.
- The load is treated as a material point.
- The drive function of the hoist winch can be assumed in two ways: as a kinematic excitation or force excitation by a given moment.
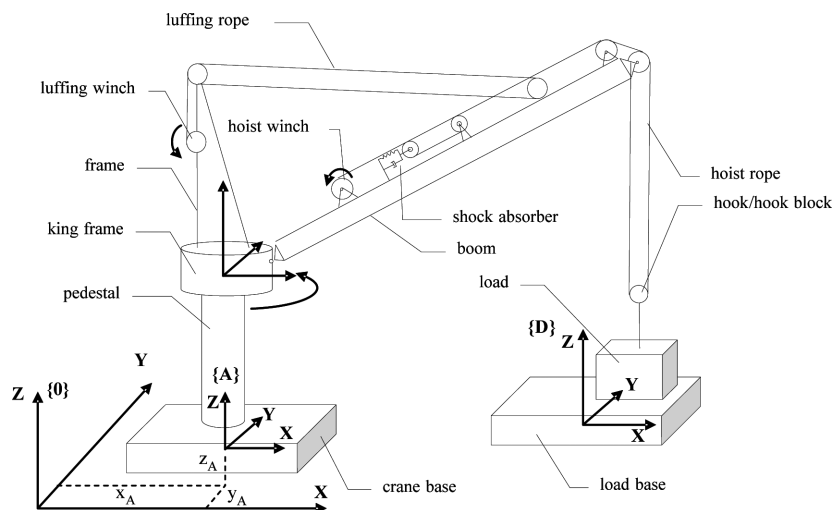- The luffing winch drive and the slew of the crane is adopted as a kinematic excitation.

Fig. 2. Scheme of the model of an offshore crane

The equations of motions are derived from the Lagrange equations of the second order:

$$\frac{d}{dt}\frac{\partial E}{\partial \dot{q}_k} - \frac{\partial E}{\partial q_k} + \frac{\partial V}{\partial q_k} + \frac{\partial D}{\partial \dot{q}_k} = Q_k \quad \text{for} \quad k = 1,\ldots,n, \qquad (1)$$

where: q_k, $\dot{q}_k$ – generalized coordinates and its velocities,

E, V – kinetic and potential energy,

D – function of energy dissipation,

Q_k – non-potential generalized force corresponding to the k-th generalized coordinate,

n – number of generalized coordinates.

For the description of the system, joint coordinates and homogenous transformations are used based on Denavit-Hartenberg notation [13, 14]. Homogeneous transformations enable succinct notation for relations describing components of Lagrange equations. In the general case, the matrix of a homogeneous transformation from coordinate system $\{i\}$ to coordinate system $\{i\text{-}1\}$ has the form:

$$
{}_{i}^{i-1}\mathbf{T} = \left[\begin{array}{cc} {}_{i}^{i-1}\mathbf{R} & {}^{i-1}\mathbf{r}_i\text{org} \\ \mathbf{0} & 1 \end{array} \right], \tag{2}
$$

where: ${}_{i}^{i-1}\mathbf{R}$ – direction cosine matrix of the axes of coordinate system $\{i\}$ relative to coordinate system $\{i\text{-}1\}$, also called slew or rotation matrix,

${}^{i-1}\mathbf{r}_i\text{org}$ – vector of coordinates of the origin of system $\{i\}$ in system $\{i\text{-}1\}$.

A vector ${}^{i}\mathbf{r}_A$ of coordinates of any point A given in system $\{i\}$ transforms to system $\{i\text{-}1\}$ according to the formula:

$$
{}^{i-1}\mathbf{r}_A = {}_{i}^{i-1}\mathbf{T} \, {}^{i}\mathbf{r}_A. \tag{3}
$$

The discussed model of a crane is described in detail, among other things, in [15]. Discussions of problems concerning modelling of the pedestal, the frame and the boom are presented below.

2.1. Crane pedestal

The crane pedestal is digitized by means of MRFEM. The number of rigid elements into which the pedestal is divided equals n_1+1. The first rigid element (rfe (1,0)) is added to the crane base. The generalized coordinates, describing the locations of the second and remaining rigid elements modelling the pedestal with respect to its predecessors, may be presented as vectors:

$$
\tilde{\mathbf{q}}^{(1,i)} = \left[\begin{array}{ccc} \varphi_x^{(1,i)} & \varphi_y^{(1,i)} & \varphi_z^{(1,i)} \end{array} \right]^T = \left[\begin{array}{ccc} \tilde{q}_x^{(1,i)} & \tilde{q}_y^{(1,i)} & \tilde{q}_z^{(1,i)} \end{array} \right]^T, \tag{4}
$$

where $\varphi_x^{(1,i)}$, $\varphi_y^{(1,i)}$, $\varphi_z^{(1,i)}$ are the rotation angles presented in Fig. 3.

The vector of generalized coordinates of the rfe is:

$$
\mathbf{q}^{(1,1)} = \tilde{\mathbf{q}}^{(1,1)} = \left[\begin{array}{ccc} q_1^{(1,1)} & q_2^{(1,1)} & q_3^{(1,1)} \end{array} \right]^T, \tag{5}
$$

$$
\mathbf{q}^{(1,i)} = \left[\begin{array}{cc} \mathbf{q}^{(1,i-1)} & \tilde{\mathbf{q}}^{(1,i)} \end{array} \right]^T = \left[\begin{array}{cccc} q_1^{(1,i)} & q_2^{(1,i)} & \ldots & q_{3i}^{(1,i)} \end{array} \right]^T \text{ for } i = 2, ..., n_1. \tag{6}
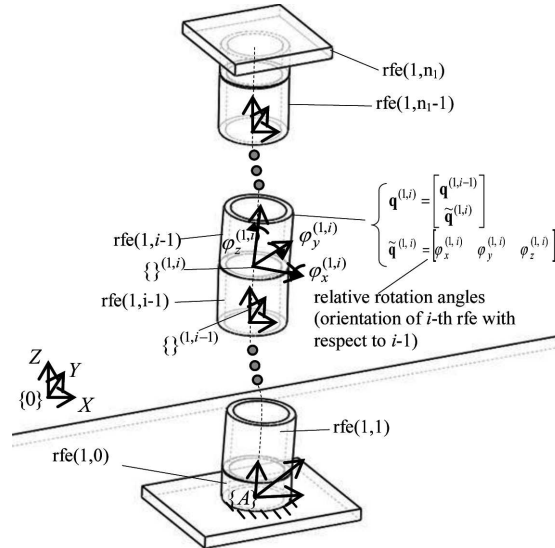$$

Fig. 3. Pedestal discretized by mean of MRFEM

In accordance to the above consideration, during the derivation of the equations of motions, kinetic and potential energy of the rfe (1,0) are omitted. The kinetic energy of the body discretized by the MRFEM may be calculated as [12]:

$$E_1 = \sum_{i=1}^{n_1} E_{(1,i)}, \tag{7}$$

where: $E_{(1,i)} = \dfrac{1}{2} tr \left\{ \dot{\mathbf{T}}^{(1,i)} \, \mathbf{H}^{(1,i)} \, \dot{\mathbf{T}}^{(1,i)^T} \right\}$,

$\mathbf{H}^{(1,i)}$ – inertia matrix of the rigid element (1,i) defined in its own coordinate system,

$\mathbf{T}^{(1,i)}$ – transformation matrix from coordinate system of rfe{1,i} into the inertial coordinate system {0},

$\mathbf{T}^{(1,i)} = \mathbf{T}^{(1,i-1)} \, \tilde{\mathbf{T}}^{(1,i)} = {}^{0}_{A}\mathbf{T} \, \tilde{\mathbf{T}}^{(1,0)} \tilde{\mathbf{T}}^{(1,1)} \cdot \ldots \cdot \tilde{\mathbf{T}}^{(1,i-1)} \, \tilde{\mathbf{T}}^{(1,i)}$ for $i = 1, .., n_1$,

$\tilde{\mathbf{T}}^{(1,i)}$ – transformation matrix from coordinate system of rfe {1,i} into system of rfe {1,i-1},

${}^{0}_{A}\mathbf{T}$ – transformation matrix from coordinate system {A} to the inertial coordinate system {0} depending on time (due to the drift motion of the crane base).

For Lagrange equations, the notion of Lagrange operators may be introduced:

$$\varepsilon_i (E) = \frac{d}{dt} \frac{\partial E}{\partial \dot{q}_i} - \frac{\partial E}{\partial q_i} \tag{8}$$

Such operators for rfes $(1,i)$ $(i =1,...,n_1)$, may be written in the vector form as:

$$\varepsilon_{\mathbf{q}^{(1,i)}}\left(E_{(1,i)}\right) = \mathbf{A}^{(1,i)}\ddot{\mathbf{q}}^{(1,i)} + \mathbf{e}^{(1,i)}, \tag{9}$$

where $\mathbf{A}^{(1,i)} = \left(a_{k,j}^{(1,i)}\right)_{k,j=1,...,3n_1} = \mathrm{tr}\left\{\mathbf{T}_k^{(1,i)}\,\mathbf{H}^{(1,i)}\,\mathbf{T}_j^{(1,i)T}\right\}$,

$$\mathbf{e}^{(1,i)} = \left(e_k^{(1,i)}\right)_{k=1,...,3n_1} = \sum_{j=1}^{3n_1}\sum_{l=1}^{3n_1} \mathrm{tr}\left\{\mathbf{T}_k^{(1,i)}\,\mathbf{H}^{(1,i)}\mathbf{T}_{j,l}^{(1,i)}\right\}\dot{q}_j^{(1,i)}\,\dot{q}_l^{(1,i)} +$$
$$+ \mathrm{tr}\left\{\mathbf{T}_k^{(1,i)}\mathbf{H}^{(1,i)}\left[{}_A^0\ddot{\mathbf{T}}\,\bar{\mathbf{T}}^{(1,i)} + 2{}_A^0\dot{\mathbf{T}}\,\dot{\bar{\mathbf{T}}}^{(1,i)}\right]^T\right\},$$

$$\bar{\mathbf{T}}^{(1,i)} = \prod_{j=0}^{i} \tilde{\mathbf{T}}^{(1,j)},$$

$$\mathbf{T}_k^{(1,i)} = \frac{\partial \mathbf{T}^{(1,i)}}{\partial q_k^{(1,i)}},$$

$$\mathbf{T}_{j,l}^{(1,i)} = \frac{\partial}{\partial q_j^{(1,i)}}\left(\frac{\partial \mathbf{T}^{(1,i)}}{\partial q_l^{(1,i)}}\right).$$

The potential energy due to gravity forces of the pedestal's rigid elements may be described by the formulae:

$$V_{(1,i)}^g = m^{(1,i)}g\,\theta_3\mathbf{T}^{(1,i)}\tilde{\mathbf{r}}_C^{(1,i)},\ \text{for } i = 1, 2, ..., n_1 \tag{10}$$

where: $m^{(1,i)}$ – mass of the rfe $(1,i)$,

g – gravity acceleration,

$\theta_3 = \begin{bmatrix} 0 & 0 & 1 & 0 \end{bmatrix}$,

$\tilde{\mathbf{r}}_C^{(1,i)}$ – vector of the element mass centre $(1,i)$ expressed in its own local coordinate system.

Corresponding derivatives, which are the elements of the Lagrange equations, are:

$$\frac{\partial V_{(1,i)}^g}{\partial \mathbf{q}^{(1,i)}} = \mathbf{G}^{(1,i)}, \tag{11}$$

where: $\mathbf{G}^{(1,i)} = \left(g_k^{(1,i)}\right)_{k=1,...,3n_1}$,

$g_k^{(1,i)} = m^{(1,i)}g\,\theta_3\mathbf{T}_k^{(1,i)}\tilde{\mathbf{r}}_C^{(1,i)}.$

In MRFEM, the consecutive rfes are connected with each other by means of massless, spring-damping elements (sde). Potential energy of elastic deformation of rfe $(1,i)$ is given as:

$$V_{(1,i)}^s = \frac{1}{2}\left(c_{i,x}^{(1)}\left[\varphi_x^{(1,i)}\right]^2 + c_{i,y}^{(1)}\left[\varphi_y^{(1,i)}\right]^2 + c_{i,z}^{(1)}\left[\varphi_z^{(1,i)}\right]^2\right) = \frac{1}{2}\sum_{j=1}^{3} c_{i,j}^{(1)}\left[\tilde{q}_j^{(1,i)}\right]^2,$$

(12)

where $c_{i,x}^{(1)}, c_{i,y}^{(1)}, c_{i,z}^{(1)}$ are the adequate coefficients of the rotational stiffness of rfe $(1,i)$.

The expression (12) may be put in the form:

$$V_{(1,i)}^s = \frac{1}{2}\tilde{\mathbf{q}}^{(1,i)T}\mathbf{C}^{(1,i)}\tilde{\mathbf{q}}^{(1,i)},$$

(13)

where $\mathbf{C}^{(1,i)} = diag\left[\begin{array}{ccc} c_{i,x}^{(1)} & c_{i,y}^{(1)} & c_{i,z}^{(1)} \end{array}\right] = diag\left[\begin{array}{ccc} c_{i,1}^{(1)} & c_{i,2}^{(1)} & c_{i,3}^{(1)} \end{array}\right]$.

The required derivatives of the potential energy of elastic deformation have a simple form:

$$\frac{\partial V_{(1,i)}^s}{\partial \tilde{\mathbf{q}}^{(1,i)}} = \mathbf{C}^{(1,i)}\tilde{\mathbf{q}}^{(1,i)}.$$

(14)

It may additionally be assumed that in rfe $(1,i)$ dissipation of the energy appears:

$$D_{(1,i)} = \frac{1}{2}\left(b_{i,x}^{(1)}\left[\dot{\varphi}_x^{(1,i)}\right]^2 + b_{i,y}^{(1)}\left[\dot{\varphi}_y^{(1,i)}\right]^2 + b_{1,z}^{(1)}\left[\dot{\varphi}_z^{(1,i)}\right]^2\right) = \frac{1}{2}\sum_{j=1}^{3} b_{1,j}^{(1)}\left[\dot{\tilde{q}}_j^{(1,i)}\right]^2,$$

(15)

where $b_{i,x}^{(1)}$, $b_{i,y}^{(1)}$, $b_{i,z}^{(1)}$ are respective damping coefficients of rfe $(1,i)$.

The equation (15) may be also written as:

$$D_{(1,i)} = \frac{1}{2}\dot{\tilde{\mathbf{q}}}^{(1,i)T}\mathbf{B}^{(1,i)}\dot{\tilde{\mathbf{q}}}^{(1,i)},$$

(16)

where $\mathbf{B}^{(1,i)} = diag\left[\begin{array}{ccc} b_{i,x}^{(1)} & b_{i,y}^{(1)} & b_{i,z}^{(1)} \end{array}\right] = diag\left[\begin{array}{ccc} b_{i,1}^{(1)} & b_{i,2}^{(1)} & b_{i,3}^{(1)} \end{array}\right]$,
and the corresponding derivatives may be obtained from:

$$\frac{\partial D_{(1,i)}}{\partial \dot{\tilde{\mathbf{q}}}^{(1,i)}} = \mathbf{B}^{(1,i)}\dot{\tilde{\mathbf{q}}}^{(1,i)}.$$

(17)

2.2. King frame, frame and boom

Let us consider the following vector of generalized coordinates for a king frame:

$$\mathbf{q}^{(2)} = \left[\begin{array}{cc} \mathbf{q}^{(1,n_k)} & \varphi_z^{(2)} \end{array}\right]^T = \left[\begin{array}{cccc} q_1^{(2)} & q_2^{(2)} & \cdots & q_{n_2}^{(2)} \end{array}\right]^T,$$

(18)

where φ_z is the angle of rotation of the king frame with respect to the pedestal.

The kinetic energy of the king frame can be described as:

$$E_2 = \frac{1}{2} tr \left\{ \dot{\mathbf{T}}^{(2)} \, \mathbf{H}^{(2)} \, \dot{\mathbf{T}}^{(2)^T} \right\},$$ (19)

where: $\mathbf{H}^{(2)}$ – the inertial matrix of the king frame,

$\mathbf{T}^{(2)}$ – transformation matrix from coordinate system {2} (connected with the king frame) into the coordinate system {0}.

The potential energy of the gravity forces equals:

$$V_2^g = m^{(2)} g \, \theta_3 \mathbf{T}^{(2)} \tilde{\mathbf{r}}_C^{(2)},$$ (20)

where: $m^{(2)}$ – mass of the king frame,

$\tilde{\mathbf{r}}_C^{(2)}$ – position vector of the centre of king frame mass, expressed in the system {2}.

The frame is modelled by means of MRFEM, considering only the flexural flexibility in the perpendicular direction to the plane of the frame (containing the frame and the boom). Additionally, like in the case of the pedestal, rfe (3,0) is added to the king frame, and as a result it does not have its own generalized coordinates – Fig. 4. The following vectors of generalized coordinates for each rfe of the frame are defined:
– one-element vectors of the flexible coordinates:

$$\tilde{\mathbf{q}}^{(3,1)} = \left[\varphi_y^{(3,1)} \right]; ...; \tilde{\mathbf{q}}^{(3,n_3)} = \left[\varphi_y^{(3,n_3)} \right]$$ (21)

– coordinate vectors describing position of the rigid element with respect to the base coordinate system:

$$\mathbf{q}^{(3,i)} = \left[\begin{array}{cccc} \mathbf{q}^{(2)T} & \tilde{\mathbf{q}}^{(3,1)T} & ... & \tilde{\mathbf{q}}^{(3,i)T} \end{array} \right]^T = \left[\begin{array}{ccc} q_1^{(3,i)} & ... & q_{n_2+i}^{(3,i)} \end{array} \right]^T \text{ for } i = 1, 2, ..., n_3$$ (22)

In contradistinction to the pedestal and frame, in the case of boom it was assumed that there is a rotational connection between the rotating part {2} and the rfe (4,0), Fig. 4 – angle ψ. The following vectors of generalized coordinates for the boom are defined:
– vectors of the flexible coordinates:

$$\tilde{\mathbf{q}}^{(4,0)} = [\psi] = \left[\varphi_y^{(4,0)} \right]; ...; \tilde{\mathbf{q}}^{(4,i)} = \left[\begin{array}{ccc} \varphi_x^{(4,i)} & \varphi_y^{(4,i)} & \varphi_z^{(4,i)} \end{array} \right]^T \text{ for } i = 1, 2, ..., n_4$$ (23)

– coordinate vectors describing position of the rigid element with respect to the base coordinate system:

$$\mathbf{q}^{(4,i)} = \left[\begin{array}{cccc} \mathbf{q}^{(2)T} & \tilde{\mathbf{q}}^{(4,0)T} & ... & \tilde{\mathbf{q}}^{(4,i)T} \end{array} \right]^T = \left[\begin{array}{ccc} q_1^{(4,i)} & ... & q_{3i+n_2+1}^{(4,i)} \end{array} \right]^T \text{ for } i = 0, 1, ..., n_4$$ (24)
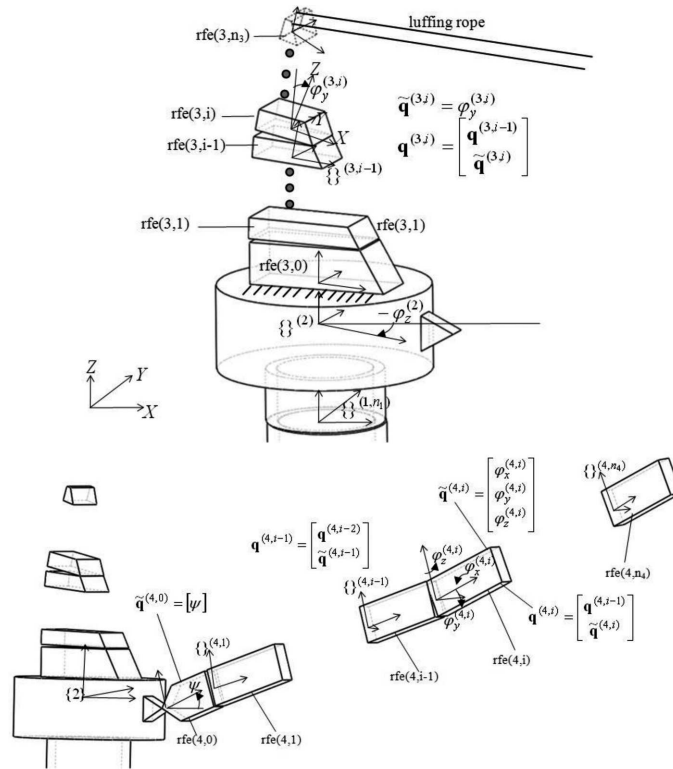
Fig. 4. Simplified model of flexible frame and boom

The necessary elements of the Lagrange equations related to the frame and boom subsystems are obtained in the same way as presented in chapter 2.1.

2.3. Hoisting and luffing ropes, load, drive systems

The potential energy of elastic deformation and function of energy dissipation of the hoist rope and luffing rope may be described by the following equations:

$$V_l = \frac{1}{2}\delta\, c^{(l)} \Delta_l^2,\tag{25}$$

$$D_l = \frac{1}{2}\delta\, b^{(l)} \dot{\Delta}_l^2,\tag{26}$$

where: $\delta = \begin{cases} 0 & \text{for } \Delta_l \le 0 \\ 1 & \text{for } \Delta_l > 0 \end{cases}$,

Δ_l – elongation of the hoist rope or luffing rope,
$c^{(l)}, b^{(l)}$ – stiffness and damping coefficients of rope, respectively.

Because of the possibility of significant changes in the active length of the hoist rope during crane operation, the stiffness coefficient of the hoist rope is determined thus:

$$c^{(l)} = \frac{E_6 F_6}{L_{6,0} - \alpha_{(6)} r_{(6)}}, \tag{27}$$

where: $L_{6,0}$ – initial length of the hoist rope,

E_6, F_6 – Young's modulus and cross section of the wire rope core, respectively,

$\alpha_{(6)}$ – rotation angle of the hoist winch drum,

$r_{(6)}$ – radius of the hoist winch drum.

The stiffness coefficient $c^{(l)}$ of the luffing rope is considered as a constant value. A method of determining the necessary derivatives of equations (25) and (26) is described in [16], which is applied in the present work as well.

The load is modelled as a material point. The weight of the hook block is added to the weight of the load. The vector of generalized coordinates is given as:

$$\mathbf{q}^{(L)} = \left[\begin{array}{ccc} x^{(L)} & y^{(L)} & z^{(L)} \end{array} \right]^T = \left[\begin{array}{ccc} q_1^{(L)} & q_2^{(L)} & q_3^{(L)} \end{array} \right]^T. \tag{28}$$

The kinetic and potential energy of the load are described by:

$$E_L = \frac{1}{2} m^{(L)} \left(\dot{x}^{(L)2} + \dot{y}^{(L)2} + \dot{z}^{(L)2} \right), \tag{29}$$

$$V_L^g = m^{(L)} g z^{(L)}, \tag{30}$$

where $m^{(L)}$ is the mass of the load.

Slewing, hoisting and luffing drive systems are modelled as kinematic inputs. Therefore, the following function is known:

$$\phi_d = \phi_d(t), \tag{31}$$

where ϕ_d denotes respectively: slewing angle, hosting winch or luffing winch rotation angle.

From the perspective of planned applications of the model presented, the hosting machinery is one of the most significant drive systems. Therefore, we apply a second method of its modelling, using forced excitation. Based on a survey of literature (for example [17]) as well as crane experience gained from crane operators and designers, the hoist winch characteristic is assumed to be as shown in Fig. 5.
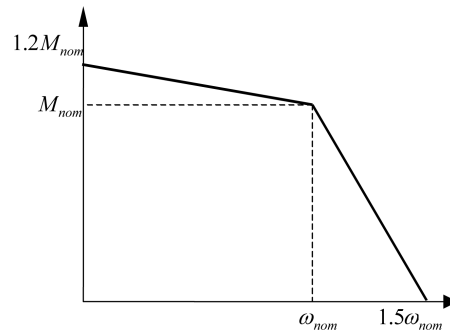
Fig. 5. Characteristics of the drive system of hoist winch drum

2.4. Aggregation of the equations of motion

Having determined the required derivatives, we may write the equations of motion of the whole crane as:

$$\mathbf{A}\,\ddot{\mathbf{q}} = \mathbf{F}\,, \tag{32}$$

where: $\mathbf{A}$ − mass matrix,

$\mathbf{F}$ − the right side vector; its elements are designated as the partial derivatives of the kinetic energy, potential forces of gravity and flexibility, partial derivatives of the function of energy dissipation and components derived from external forces.

The equations (32) were solved by a computer programme using the fourth order Runge-Kutta method with fixed step integration. Before the integration of (32), initial conditions were calculated by solving the proper static problem. The resulting system of nonlinear algebraic equations was solved using the Newton's method. A convenient user interface (Fig. 6) was designed to facilitate initial analysis of yielded results.
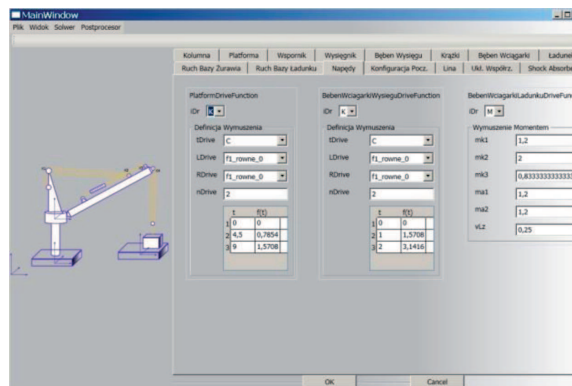
Fig. 6. Sample screenshot of the user interface

3. Numerical simulations

The method of modelling a crane's supporting structure using MRFEM presented in chapter 2 allows us to conveniently perform analyses in order to determine the influence of flexibilities of individual structural components (pedestal, frame, boom) on the device's dynamics. The current chapter exemplifies such considerations.

The computations are performed for a case of lifting a load from a motionless supply vessel (a wharf) with movable base of the crane. The mass of the lifted load is 10 000 kg. The rope (initially lax) is assumed to have 0.75 m excess in length and the lifting speed to be 0.7 m/s with gear in the lifting system equal 2. The hoist winch drum is forced to rotate by a moment. The characteristics of the drive system are presented in Fig. 5. The geometric-mass parameters correspond to OC3500 class crane. The pedestal height is 31.9 m, the frame nearly 15 m and the boom is about 59 m long. Motion of the base occurs only in the direction of the Z axis (plunging) and is determined, as in [18], by the function:

$$z_P = 1,2\left(\sin\left(0,52t + 1,57\right) + \frac{1}{4}\sin\left(1,04t + 1,57\right) + \frac{1}{9}\sin\left(1,56t + 1,57\right)\right) \; [m]. \quad (33)$$

The following notation is assumed in the graphs: KxWyJz, where x, y, z denotes the numbers of ests present in the discretized components, namely in the pedestal (K), the frame (W) and the boom (J), respectively. A number est = 0 means that a given component is modelled as a rigid one. In all the cases presented below, flexibility of the hoist rope is taken into consideration, since the authors' experience indicates that it is the element of the crane whose flexibility has the most influence of the device's dynamics. One of the compared values is the dynamic overload coefficient in the hoist rope defined as:

$$\eta = \frac{S_L}{m_L \, g}. \quad (34)$$

where: S_L – hoist rope force,
   m_L – mass of the load.

In the first stage of the analysis, the number of ests in each of the discretized components is changed simultaneously. Figs. 7a) and 7b), respectively, show the z coordinate of the load and its second derivative, and Fig. 8 the dynamic coefficient η, both with respect to time.

The figures above present that flexibilities of the crane components have a slight influence on coordinate z. Their importance grows in analyses related to second derivatives of coordinate z or the dynamic coefficient.

Subsequent analyses investigate the influence of taking into account flexibilities of individual components of the crane, assuming that only one of
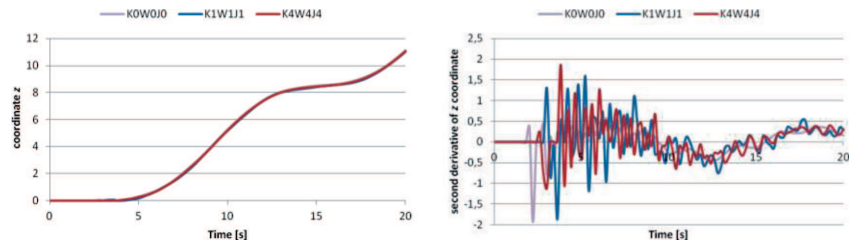
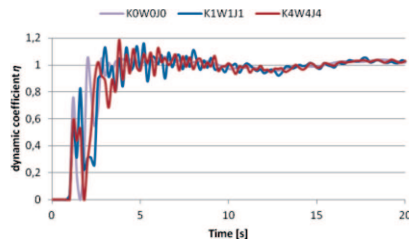Fig. 7. Time courses of: a) the z coordinate of the load b) its second derivative

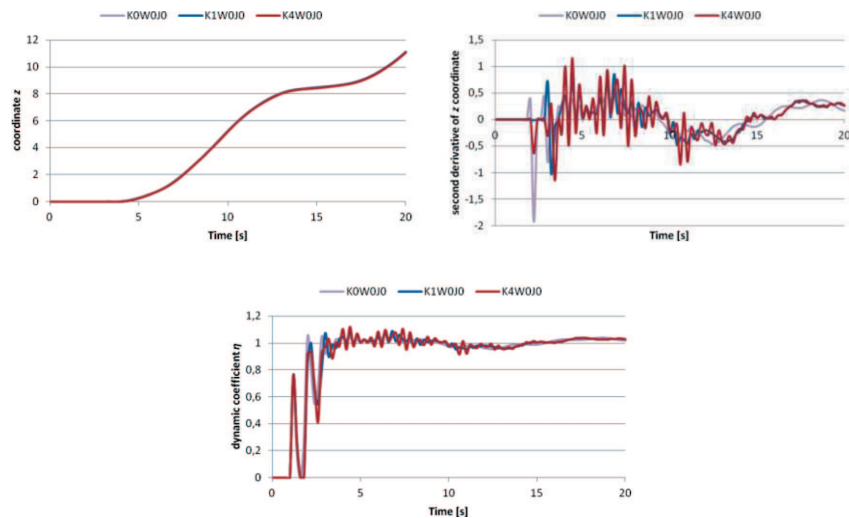Fig. 8. Graph of the dynamic coefficient η in the function of time

Fig. 9. Graphs of time functions, assuming a flexible pedestal, of: a) the z coordinate of the load
b) its second derivative c) the dynamic coefficient η

them is flexible. The graphs in Fig. 9 are for a flexible pedestal. More results, including ones for flexible boom and frame, can be found in [19].

4. Modelling a pedestal with rigid finite elements of variable length

A custom approach with rigid finite elements of variable length, developed in search for methods of modelling components of a crane which are as efficient computationally as possible, is described below. Fig. 10 portrays
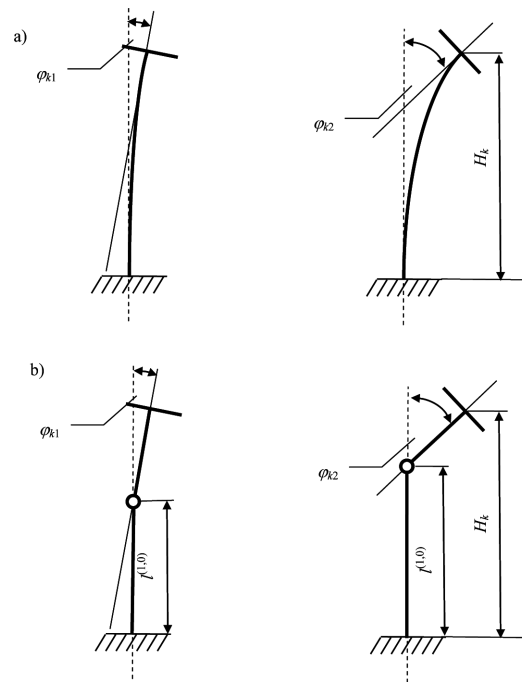
Fig. 10. Modelling a pedestal

the idea for a flat problem. In Fig. 10a), there are presented two cases of deflection of a pedestal modelled as a continuous system. The angle φ_k is relevant to the position of the slewing part of the crane based on the pedestal. The proposed model (Fig. 10b) consists of two rigid components connected by an est. Their lengths (in particular the length $l^{(1,0)}$ of the first component, fixed to a movable base) vary with the angle φ_k. The stiffness coefficient of the est simultaneously undergoes a change. These parameters (length of the ses and stiffness coefficient of the est), called equivalent parameters, are chosen in such way that the total length H_k of the pedestal be preserved and the angle between the components equal φ_k.

4.1. Determining equivalent parameters for a pedestal model with FEM

A simplified model of a pedestal was developed using FEM in order to determine its equivalent parameters. The FEM analysis enables determining the inclination angle φ_k of the upper surface of the pedestal and its horizontal displacement ΔU_y depending on load. This gives the ability to determine the equivalent parameters for the pedestal model, which may be used in a model of an entire crane.

A geometric model of a sample pedestal was created using the programme Inventor 2008 – Fig. 11. It was subsequently imported into the

Ansys Workbench 11 environment in which the FEM model was developed. It consists of 45970 8-node solid elements (solid type 185) and 72930 nodes.
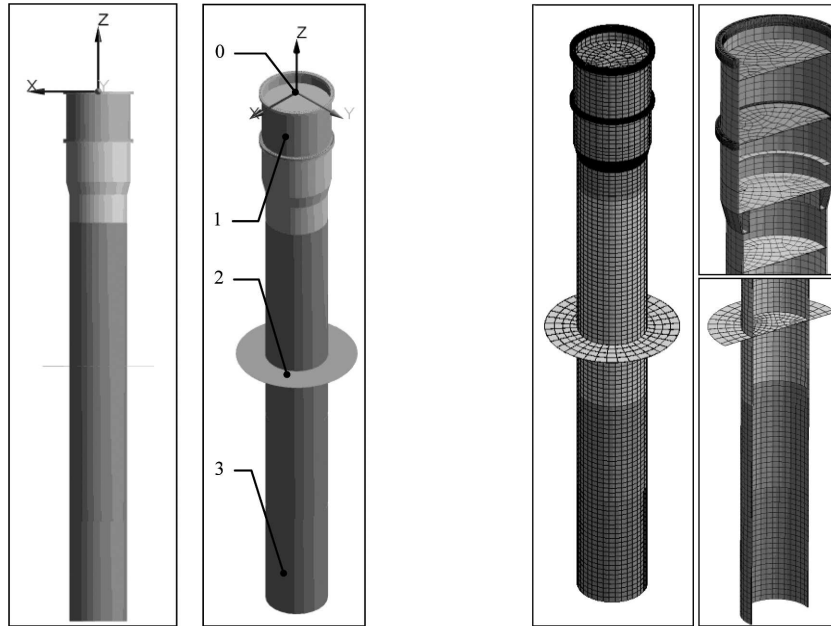

Fig. 11. Crane pedestal, geometric model and FEM model

Static analysis of the pedestal is performed for the applied bending moment of $M_k = 40\ 000$ kNm (around the global X axis). This moment is mainly due to the load on the crane's hook. Table 1 presents the results of FEM computations. They comprise twenty substeps. The analysis yields the displacements caused by the bending moment M_k:

ΔU_y – horizontal displacement of the centre of pedestal upper flange,

ΔU_z – vertical displacement of the pedestal upper flange.

The values of dislocations determined by FEM analysis are used to compute the equivalent parameters of the pedestal model – Fig. 12. The angle φ_k caused by the action of the bending moment M_k is determined by:

$$\phi_k = \arcsin\left(\frac{\Delta U_z}{r}\right). \tag{35}$$

where r is the external radius of the pedestal upper flange.

Length $l^{(1,0)}$ of a rigid element depends on the angle φ_k:

$$l^{(1,0)} = H_k - \frac{\Delta U_y}{\operatorname{tg}(\varphi_k)} \tag{36}$$

where H_k is the overall height of the pedestal.
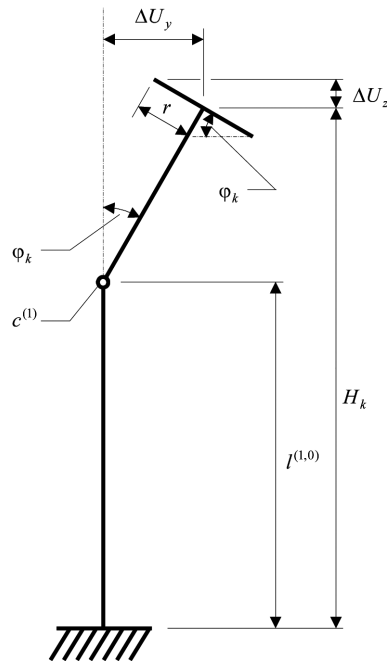
Fig. 12. Equivalent model

Stiffness coefficient of an est is determined from the relation:

$$c^{(1)} = \frac{M_k}{\varphi_k}.\tag{37}$$

4.2. Examples of computations

Results of computations for a sample pedestal of height 39.1 m and diameter of the upper part 3.54 m are shown below. Table 1 presents the results of FEM computations and the equivalent parameters.

The described simplified model of a pedestal was implemented in the main computer programme, enabling comparison of the results obtained for both modelling methods. Selected results of numerical simulations are presented below, and conclusions are drawn about the usefulness of an equivalent pedestal model. A case of a crane subjected to undulation is considered, whereby only plunging is taken into account, defined as:

$$z^{(A)} = 1,5 \sin\left(\frac{2\pi_z}{8}\right)t[\text{m}],\tag{38}$$

Mass of load, assumed in the simulations, equals 10000 kg. The boom is positioned horizontally. The computations are done under the assumption

Table 1.

Results of FEM a computations and values of equivalent parameters for a sample pedestal

No.	% max value	M_k [kNm]	ΔU_y [m]	ΔU_z [m]	φ_k [deg]	$l^{(1,0)}$ [mm]	$c^{(1,0)}$ [N/m]
1	5	2 000	$4.25 \cdot 10^{-3}$	$0.52 \cdot 10^{-3}$	0.02	16 124	$5.73 \cdot 10^6$
2	10	4 000	$8.50 \cdot 10^{-3}$	$1.32 \cdot 10^{-3}$	0.04	19 420	$5.73 \cdot 10^6$
3	15	6 000	$12.75 \cdot 10^{-3}$	$2.13 \cdot 10^{-3}$	0.06	20 232	$5.73 \cdot 10^6$
4	20	8 000	$17.00 \cdot 10^{-3}$	$2.93 \cdot 10^{-3}$	0.09	20 600	$5.09 \cdot 10^6$
5	25	10 000	$21.25 \cdot 10^{-3}$	$3.73 \cdot 10^{-3}$	0.11	20 811	$5.21 \cdot 10^6$
6	30	12 000	$25.50 \cdot 10^{-3}$	$4.53 \cdot 10^{-3}$	0.13	20 946	$5.29 \cdot 10^6$
7	35	14 000	$29.74 \cdot 10^{-3}$	$5.33 \cdot 10^{-3}$	0.16	21 041	$5.01 \cdot 10^6$
8	40	16 000	$33.99 \cdot 10^{-3}$	$6.13 \cdot 10^{-3}$	0.18	21 111	$5.09 \cdot 10^6$
9	45	18 000	$38.24 \cdot 10^{-3}$	$6.93 \cdot 10^{-3}$	0.20	21 165	$5.16 \cdot 10^6$
10	50	20 000	$42.49 \cdot 10^{-3}$	$7.73 \cdot 10^{-3}$	0.23	21 208	$4.98 \cdot 10^6$
11	55	22 000	$46.74 \cdot 10^{-3}$	$8.53 \cdot 10^{-3}$	0.25	21 242	$5.04 \cdot 10^6$
12	60	24 000	$50.99 \cdot 10^{-3}$	$9.33 \cdot 10^{-3}$	0.27	21 271	$5.09 \cdot 10^6$
13	65	26 000	$55.24 \cdot 10^{-3}$	$10.13 \cdot 10^{-3}$	0.30	21 295	$4.97 \cdot 10^6$
14	70	28 000	$59.49 \cdot 10^{-3}$	$10.93 \cdot 10^{-3}$	0.32	21 316	$5.01 \cdot 10^6$
15	75	30 000	$63.74 \cdot 10^{-3}$	$11.73 \cdot 10^{-3}$	0.35	21 333	$4.91 \cdot 10^6$
16	80	32 000	$67.99 \cdot 10^{-3}$	$12.53 \cdot 10^{-3}$	0.37	21 349	$4.96 \cdot 10^6$
17	85	34 000	$72.24 \cdot 10^{-3}$	$13.33 \cdot 10^{-3}$	0.39	21 363	$5.00 \cdot 10^6$
18	90	36 000	$76.49 \cdot 10^{-3}$	$14.13 \cdot 10^{-3}$	0.42	21 375	$4.91 \cdot 10^6$
19	95	38 000	$80.73 \cdot 10^{-3}$	$14.94 \cdot 10^{-3}$	0.44	21 386	$4.95 \cdot 10^6$
20	100	40 000	$84.98 \cdot 10^{-3}$	$15.74 \cdot 10^{-3}$	0.46	21 396	$4.98 \cdot 10^6$

that the frame and boom are rigid components. The following denotations are used in the graphs:

zast – computations according to the equivalent pedestal model described in this chapter,

cyl_0 – pedestal treated as a rigid component,

cyl_1 – pedestal discretized using two rigid finite elements,

cyl_3 – pedestal discretized using four rigid finite elements.

The presented graphs indicate significant influence of pedestal flexibility on dynamics of an entire crane. The cases in which the pedestal is treated as a rigid component lead to results somewhat different to those when its flexibility is considered. Particularly marked are the differences in force in the rope. The method of modelling flexibility and the number of rigid finite
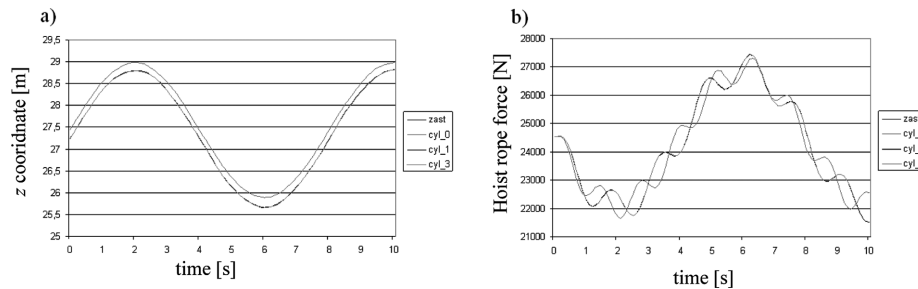
a)   b)

Fig. 13. Comparison of the MFEM model to the equivalent model a) the z coordinate of the load
b) hoist rope force

elements discretizing the pedestal make almost no difference, however. Also, the obtained results confirm adequacy of the modified method of modelling a pedestal. Computation times were compared for particular cases to determine if it is computationally more efficient. The following durations [mm:ss] were obtained on a computer equipped with Duo CPU P8600 @ 2.40GHz, 4.0GB RAM and a 32-bit operating system:

    zast – 1:23,
    cyl_0 – 0:51,
    cyl_1 – 1:25,
    cyl_3 – 3:57.

The most interesting feature is how the time durations for „zast" and „cyl_1" compared (they both have 1 est), being almost equal. Since the obtained results are also nearly identical, it seems that the use of the modified method of modelling a pedestal does not bring the expected outcome in the form of significant increase of the model's numerical efficiency. The fact that determining equivalent parameters of the model is costly should also be recalled, further favouring the classical rigid finite element method.

5. Conclusions

The presented results of numerical simulations confirm adequacy of using MRFEM to model an offshore pedestal crane. Depending on the problem considered, flexibilities of main structural components: the pedestal, the frame and the boom, can be taken into account or omitted. The analysis of the obtained graphs shows that the flexibilities hardly influence the dependency of the load's coordinates on time. This allows for using simplified models with few degrees of freedom to perform computations for purposes of marketing or related to control. On the other hand, considering the flexibilities makes it possible to perform more complex analyses related to the dynamics of individual subsystems of the crane. Depending on the number of finite

elements assumed in modelling, the phenomena occurring with vibrations of higher frequencies can be analysed.

As a formulation of conclusions from the computations discussed in chapter 4, it can be stated that for many cases of dynamic analyses of an offshore pedestal crane it is enough to use two rigid finite elements to model the crane pedestal, since increasing their number does not cause significant differences in obtained results. Note that these conclusions pertain to one sample structure of a pedestal. For pedestals with different geometric-mass parameters it is always worthwhile to check what number of ses should be used to discretize them in order for the results to be satisfactory. If the analyses require more ses, the method proposed herein may prove competitive.

REFERENCES

[1] Pedrazzi C., Barbieri G., LARSC: Launch and recovery smart crane for naval ROV handling, 13th European ADAMS Users' Conference, Paris, 1998.

[2] Adamiec-Wójcik I., Fałat P., Maczyński A., Wojciech S.: Load stabilisation an A-frame – a type of an offshore crane, The Archive of Mechanical Engineering, Vol. 56, No 1, pp. 37-59, 2009.

[3] Urbaś A., Szczotka M., Maczyński A.: Analysis of movement of the BOP crane under sea weaving conditions, Journal of Theoretical and Applied Mechanics, 48, pp. 677-70, 2010.

[4] Ellermann K., Kreuzer E.: Nonlinear dynamics in the motion of floating cranes, Multibody System Dynamics, 9, 4, pp. 377-387, 2003.

[5] Ellermann K., Kreuzer E., Markiewicz M.: Nonlinear primary resonances of a floating crane, Meccanica, 38, pp. 5-18, 2003.

[6] Osiński M., Wojciech S.: Application of nonlinear opitmisation methods to input shaping of the hoist drive of an off-shore crane, Nonlinear Dynamics, 17, pp. 369-386, 1998.

[7] Li Y.Y., Balachandran B.: Analytical study of a system with a mechanical filter, Journal of Sound and Vibration, 247, 633-653, 2001.

[8] Masoud Z.N., Nayfeh A.H., Mook D.T.: Cargo pendulation reduction of ship-mounted cranes, Nonlinear Dynamics, Vol. 35, No. 3, pp. 299-311, 2004.

[9] Masoud Y.N.: A control system for the reduction of cargo pendulation of ship-mounted cranes, Virginia Polytechnic Institute and State University. PhD Thesis, Blacksburg, Virginia, 2000.

[10] Maczyński A., Wojciech S.: Stabilization of load's position in offshore cranes, Journal of Offshore Mechanics and Arctic Engineering, Vol. 134, pp. 1-10, 2012.

[11] Schaub H.: Rate-based ship-mounted crane payload pendulation control system, Control Engineering Practice, 16, pp. 132-145, 2008.

[12] Wittbrodt E., Szczotka M., Maczyński A., Wojciech S.: Rigid Finite Element Method in Analysis of Dynamics of Offshore Structures. Springer, 2013.

[13] Craig J.J.: Introduction to Robotics, Prentice Hall, 3 edition, 2004.

[14] Adamiec-Wójcik I., Maczyński A., Wojciech S.: Zastosowanie metody przekształceń jednorodnych w modelowaniu dynamiki urządzeń offshore (Application of homogeneous transformation method for modeling the dynamics of offshore structures), Wydawnictwa Komunikacji i Łączności, Warszawa, 2008 (in Polish).